The Journal of Experimental Biology 206, 2059-2072

doi:10.1242/jeb.00242



## Review

# Metabolic consequences of functional complexes of mitochondria, myofibrils and sarcoplasmic reticulum in muscle cells

T. Andrienko[1,2], A. V. Kuznetsov[1,3], T. Kaambre[4], Y. Usson[5], A. Orosco[1], F. Appaix[1], T. Tiivel[4], P. Sikk[4], M. Vendelin[6], R. Margreiter[3] and V. A. Saks[1,4,*]

[1]*Laboratory of Fundamental and Applied Bioenergetics, INSERM E0221, Joseph Fourier University, Grenoble, France,* [2]*A. N. Belozersky Institute of Physico-Chemical Biology, Moscow State University, Moscow, Russia,* [3]*Department of Transplant Surgery, University Hospital Innsbruck, Innsbruck, Austria,* [4]*Laboratory of Bioenergetics, National Institute of Chemical Physics and Biophysics, Tallinn, Estonia,* [5]*RFMQ-TIMC Laboratory, UMR 5525 CNRS, Institute Albert Bonniot, Grenoble, France* and [6]*Institute of Cybernetics, Tallinn, Estonia*

*Author for correspondence (e-mail: valdur.saks@ujf-grenoble.fr)

*Accepted 14 January 2003*

**Summary**

**Regulation of mitochondrial respiration both by endogenous and exogenous ADP in the cells *in situ* was studied in isolated and permeabilized cardiomyocytes, permeabilized cardiac fibers and 'ghost' fibers (all with a diameter of 10–20 μm) at different (0–3 μmol $l^{-1}$) free $Ca^{2+}$ concentrations in the medium. In all these preparations, the apparent $K_m$ of mitochondrial respiration for exogenous ADP at free $Ca^{2+}$ concentrations of 0–0.1 μmol $l^{-1}$ was very high, in the range of 250–350 μmol $l^{-1}$, in contrast to isolated mitochondria *in vitro* (apparent $K_m$ for ADP is approximately 20 μmol $l^{-1}$). An increase in the free $Ca^{2+}$ concentration (up to 3 μmol $l^{-1}$, which is within physiological range), resulted in a very significant decrease of the apparent $K_m$ value to 20–30 μmol $l^{-1}$, a decrease of $V_{max}$ of respiration in permeabilized intact fibers and a strong contraction of sarcomeres. In ghost cardiac fibers, from which myosin was extracted but mitochondria were intact, neither the high apparent $K_m$ for ADP (300–350 μmol $l^{-1}$) nor $V_{max}$ of respiration changed in the range of free $Ca^{2+}$ concentration studied, and no sarcomere contraction was observed. The exogenous-ADP-trapping system (pyruvate kinase + phosphoenolpyruvate) inhibited endogenous-ADP-supported respiration in permeabilized cells by no more than 40%, and this inhibition was reversed by creatine due to activation of mitochondrial creatine kinase. These results are taken to show strong structural associations (functional complexes) among mitochondria, sarcomeres and sarcoplasmic reticulum. Inside these complexes, mitochondrial functional state is controlled by channeling of ADP, mostly *via* energy- and phosphoryl-transfer networks, and apparently depends on the state of sarcomere structures.**

Key words: mitochondria, myofibril, sarcoplasmic reticulum, cardiomyocyte, mitochondrial respiration, muscle, intracellular energetic unit.

## Introduction

In spite of intensive studies, the intracellular mechanisms of regulation of mitochondrial function in heart and skeletal muscle are still obscure. One of the interesting observations in this area, made in numerous laboratories, is that in permeabilized oxidative muscle cells the apparent $K_m$ for exogenous ADP in the control of mitochondrial respiration is very high, in the range of 200–300 μmol $l^{-1}$, in contrast to permeabilized fibers from fast-twitch skeletal muscles and isolated mitochondria *in vitro*: in both cases, the apparent $K_m$ for ADP is 15–20 μmol $l^{-1}$ (Anflous et al., 2001; Boudina et al., 2002; Braun et al., 2001; Burelle and Hochachka, 2002; Dos Santos et al., 2002; Fontaine et al., 1995; Kay et al., 1997; Kummel, 1988; Kuznetsov et al., 1996; Liobikas et al., 2001; Milner et al., 2000; Saks et al., 1991, 1993, 1994, 1995, 1998a, 2001; Seppet et al., 2001; Toleikis et al., 2001; Veksler et al., 1995). A trivial explanation of this phenomenon by formation of ADP concentration gradients between the medium and the core of the cells is excluded (Kay et al., 1997), since the Brownian movement of adenine nucleotides in water solution across the diffusion distance of <10 μm (permeabilized cardiomyocytes) is more rapid than the metabolic turnover of ADP and ATP (Saks et al., 2001). Besides, this trivial explanation is in conflict with the tissue specificity of the phenomenon mentioned above (Kuznetsov et al., 1996; Veksler et al., 1995). Another important recent observation is that the kinetics of regulation of mitochondrial respiration in

permeabilized oxidative muscle cells is very different for exogenous and endogenous ADP (Saks et al., 2001; Seppet et al., 2001). Similarly, endogenous ATP has been shown to be a much more effective substrate for the $Ca^{2+}$-ATPase of the sarcoplasmic reticulum than is exogenous ATP (Kaasik et al., 2001). These data have led to the hypothesis of the existence of functional complexes among mitochondria, sarcoplasmic reticulum and myofibrils [intracellular energetic units (ICEUs)] as a basic pattern of organization of energy metabolism in cardiac and oxidative muscle cells (Saks et al., 2001). Most of these studies were performed for pCa=7.0, which corresponds to the resting state of the cells (pCa=–log[$Ca^{2+}$]). In the present study, we investigated the metabolic consequences of ICEUs for the entire physiological range of free calcium concentration (0–3 μmol $l^{-1}$). The results show very strong structural associations among mitochondria, sarcomeres and sarcoplasmic reticulum, and, inside these complexes, mitochondrial functional state apparently depends on the state of the sarcomere and related structures. This structural organization results in heterogeneity of the intracellular diffusion of ADP and intracellular compartmentation of adenine nucleotides. Functioning of ICEUs is based on regulation of energy metabolism both by local concentrations and by channeling of ADP and ATP, mostly *via* energy- and phosphoryl-transfer networks.

## Materials and methods

### *Animals*

Wistar rats (*Rattus Norvegicus* L.) were used in all experiments. The investigation conforms to the *Guide for the Care and Use of Laboratory Animals* (National Institutes of Health, 1985).

### *Isolation of mitochondria from cardiac muscle*

Mitochondria were isolated from the hearts of Wistar female rats as described previously (Saks et al., 1975).

### *Isolation and culturing of adult cardiac myocytes*

Male Wistar rats weighing 300–350 g were used in all experiments. Calcium-tolerant myocytes were isolated by perfusion with a collagenase-containing medium as described previously (Kay et al., 1997).

### *Preparation of skinned and 'ghost' cardiac muscle fibers*

Skinned (permeabilized) fibers were prepared from rat cardiac muscle and m. soleus according to the method described previously (Saks et al., 1998a).

### *Determination of the rate of mitochondrial respiration in isolated mitochondria, permeabilized cardiomyocytes, skinned and 'ghost' fibers*

The rates of oxygen uptake were recorded by using the two-channel high-resolution respirometer (Oroboros Oxygraph, Paar KG, Graz, Austria) or a Yellow Spring Clark oxygen electrode (Yellow Spring, OH, USA) in solution B, with different free calcium concentrations, containing respiratory substrates (see below) and 2 mg $ml^{-1}$ bovine serum albumin (BSA). Determinations were carried out at 25°C, and solubility of oxygen was taken as 215 nmol $ml^{-1}$ (Kuznetsov et al., 1996). The method of calculation of free calcium concentration in solution B is given below.

### *Confocal microscopy*

#### *Imaging of mitochondria*

Isolated saponin-permeabilized cardiomyocytes or fibers were fixed in a flexiperm chamber (Heraeus, Hanau, Germany) with microscopic glass slide. 200 μl of respiration medium was then immediately added to the chamber. A fully oxidized state of mitochondrial flavoproteins was achieved by substrate deprivation and equilibration of the medium with air. To analyze mitochondrial calcium, isolated cardiomyocytes or permeabilized myocardial fibers were preloaded with fluorescent $Ca^{2+}$-specific probe Rhod-2 (Sigma, St Louis, MO, USA). For this, cells or fibers were incubated for 30 min at room temperature in solution B (see Solutions) with freshly added 5 μmol $l^{-1}$ Rhod-2. Rhod-2 has a net positive charge, allowing its accumulation in mitochondria. The fluorescence of Rhod-2 in loaded myocytes or fibers was excited with a 543 nm helium–neon laser. The laser output power was set to a mean power of 1 mW. Rhod-2 fluorescence and flavoproteins auto-fluorescence were imaged using a confocal microscope (LSM510NLO; Zeiss, Jena, Germany) with a 40× water immersion lens (NA 1.2). The use of such a water immersion lens prevented geometrical aberrations when observing living cells. For co-localization studies of mitochondria and mitochondrial redox potential analysis, the autofluorescence of flavoproteins was excited with the 488 nm line of an argon laser. The laser output power was set to a mean power of 8 mW. The fluorescence signals were collected through a multi-line beam splitter with maximum reflections at 488±10 nm (for rejection of the 488 nm line) and at 543 nm (for rejection of the 543 nm line). A second 545 nm beam splitter was used to discriminate the Rhod-2 signal from the flavoproteins signal. The flavoproteins signal was then passed through a 505 nm long-pass filter before being collected through a pinhole (one Airy disk unit). The Rhod-2 signal was redirected to a 560 nm long-pass filter before being collected through a pinhole (one Airy disk unit).

To analyze mitochondrial distribution and mitochondrial inner membrane potential, myocytes or fibers were incubated for 30 min at room temperature with 50 nmol $l^{-1}$ tetramethylrhodamine ethyl ester (TMRE) added to solution B. Imaging of TMRE fluorescence was performed as described for imaging of mitochondrial calcium. In control experiments, dissipation of membrane potential was observed after addition of 5 μmol $l^{-1}$ antimycin A, 4 μmol $l^{-1}$ carbonyl cyanide *p*-trifluoromethoxyphenylhydrazone (FCCP) and 0.5 μmol $l^{-1}$ rotenone.

#### *Immunofluorescence confocal microscopy*

For labelling of a cytoskeletal network in permeabilized fibers, monoclonal antibodies against β-tubulin were used. Cells were first washed in solution B before being fixed with

methanol for 5 min at –20°C. Cardiomyocytes or fibers were washed with phosphate-buffered saline (PBS; Biomedia, Boussens, France) and incubated in 2% (w/v) bovine serum albumin (BSA) in PBS overnight at 4°C with primary monoclonal antitubulin antibody (Sigma) at a 1/200 dilution. After washes in PBS, cells were incubated for 3 h in 2% (w/v) PBS/BSA with secondary antibody rhodamine tetramethyl rhodamine isothiocyanate (TRITC)-conjugated AffiniPure $F(ab')_2$ fragment donkey anti-mouse IgG at a dilution of 1/50 (Interchim, Montluçon, France). Cardiomyocytes or fibers were then washed once in PBS and three times in water. The labelled cells were deposited on glass cover slips and mounted in a mixture of Mowiol® and glycerol to which 1,4-diazabicyclo-[2,2,2]-octane (Acros Organics, Pittsburgh, PA, USA) was added to delay photobleaching. Samples were observed by confocal microscopy (LSM510 NLO; Zeiss) with a plan apo 40× oil immersion objective lens (NA 1.4).

### *Determination of pyruvate kinase activity*

The activity of pyruvate kinase (PK) in stock solutions was assessed at 25°C by a coupled lactate dehydrogenase system. The decrease in NADH level, in response to the addition of different amounts of PK, was determined spectrophotometrically in Uvikon 941 plus (Kontron Instruments, Hertfordshire, UK) in solution B supplemented with 0.3 mmol $l^{-1}$ NADH, 1 mmol $l^{-1}$ phosphoenolpyruvate (PEP), 2 mmol $l^{-1}$ ADP and 4–5 i.u. $ml^{-1}$ lactate dehydrogenase .

### *Protein concentration determination*

Protein concentration in mitochondrial preparations was determined by enzyme-linked immunosorbent assay (ELISA) using the $EL_x800$ universal microplate reader (Bio-Tek Instruments, Winooski, VT, USA) and a BSA kit (protein assay reagent) from Pierce (Rockford, IL, USA).

### *Solutions*

Composition of the solutions used for preparation of skinned fibers and for oxygraphy was based on the information of the ionic content in the muscle cell cytoplasm (Godt and Maughan, 1988).

*Solution A*

1.9 mmol $l^{-1}$ $CaK_2EGTA$, 8.1 mmol $l^{-1}$ $K_2EGTA$, 9.5 mmol $l^{-1}$ $MgCl_2$, 0.5 mmol $l^{-1}$ dithiothreitol (DTT), 50 mmol $l^{-1}$ potassium 2-(*N*-morpholino)ethanesulfonate (K-Mes), 20 mmol $l^{-1}$ imidazole, 20 mmol $l^{-1}$ taurine, 2.5 mmol $l^{-1}$ $Na_2ATP$, 15 mmol $l^{-1}$ phosphocreatine, adjusted to pH 7.1 at 25°C.

*Solution B*

1.9 mmol $l^{-1}$ $CaK_2EGTA$, 8.1 mmol $l^{-1}$ $K_2EGTA$, 4.0 mmol $l^{-1}$ $MgCl_2$, 0.5 mmol $l^{-1}$ DTT, 100 mmol $l^{-1}$ K-Mes, adjusted to pH 7.1 at 25°C, 20 mmol $l^{-1}$ imidazole, 20 mmol $l^{-1}$ taurine, 3 mmol $l^{-1}$ $K_2HPO_4$. For oxygraphy, 5 mmol $l^{-1}$ pyruvate (or 5 mmol $l^{-1}$ glutamate) and 2 mmol $l^{-1}$ malate were added as respiratory substrates.

*Solution KCl*

125 mmol $l^{-1}$ KCl, 20 mmol $l^{-1}$ Hepes, 4 mmol $l^{-1}$ glutamate, 2 mmol $l^{-1}$ malate, 3 mmol $l^{-1}$ Mg-acetate, 5 mmol $l^{-1}$ $KH_2PO_4$, 0.4 mmol $l^{-1}$ EGTA and 0.3 mmol $l^{-1}$ DTT, adjusted to pH 7.1 at 25°C, and 2 mg $ml^{-1}$ of BSA was added.

### *Reagents*

All reagents were purchased from Sigma (USA) except ATP and ADP, which were obtained from Boehringer (Mannheim, Germany).

### *Analysis of the experimental results*

The values in tables and figures are expressed as means ± S.D. The apparent $K_m$ for ADP was estimated from a linear regression of double-reciprocal plots. Statistical comparisons were made using analysis of variance (ANOVA) and the Fisher test, and $P<0.05$ was taken as the level of significance.

### *Calculations and modeling*

*Calculation of free $Ca^{2+}$ concentration*

Calculations of the composition of EGTA-Ca buffer were made according to Fabiato and Fabiato (1979), first for a total calcium concentration of 1.878 mmol $l^{-1}$. For our calculations, dissociation constants of complexes of $Mg^{2+}$ with ADP and ATP were taken from Phillips et al. (1966) and Saks et al. (1975). 10 mmol $l^{-1}$ EGTA and 2.26 mmol $l^{-1}$ ATP were used as ligand concentrations, and 9.5 mmol $l^{-1}$ magnesium and 1.878 mmol $l^{-1}$ or 2.77 mmol $l^{-1}$ calcium were used for metals for calculations for solution A. For solution B, we replaced 2.26 mmol $l^{-1}$ ATP with 1 mmol $l^{-1}$ ADP, decreased the concentration of magnesium to 4 mmol $l^{-1}$ and added 3 mmol $l^{-1}$ phosphate. In the case of the 1.878 mmol $l^{-1}$ total calcium concentration, the concentration of free calcium was found to be $1.11\times10^{-7}$ mol $l^{-1}$ for solution A and $1.04\times10^{-7}$ mol $l^{-1}$ for solution B . In the case of the 2.77 mmol $l^{-1}$ total calcium concentration, the concentration of free calcium was found to be $1.84\times10^{-7}$ mol $l^{-1}$ for solution A and $1.72\times10^{-7}$ mol $l^{-1}$ for solution B, confirming our previous rough predictions.

To increase the free calcium concentration up to 3 μmol $l^{-1}$, the total EGTA concentration in solution B was kept constant at 10 mmol $l^{-1}$ and total calcium concentration was increased by adding calculated aliquots of a stock solution of 270 mmol $l^{-1}$ $CaCl_2$. The necessary total calcium concentrations for achieving corresponding free calcium concentrations were calculated using the WINMAXC program (Stanford University, Stanford, CA, USA) according to the scheme described above. Analysis of the calculations allowed us also to use a simpler empirical formula:

$$[Ca]_{total} = \frac{a\times[Ca]_{free}}{b+[Ca]_{free}}, \quad (1)$$

where a=10.0945±0.01406 and b=0.4574±0.0021; for these coefficients, $[Ca]_{free}$ is given in μmol $l^{-1}$ and $[Ca]_{total}$ is given in mmol $l^{-1}$.

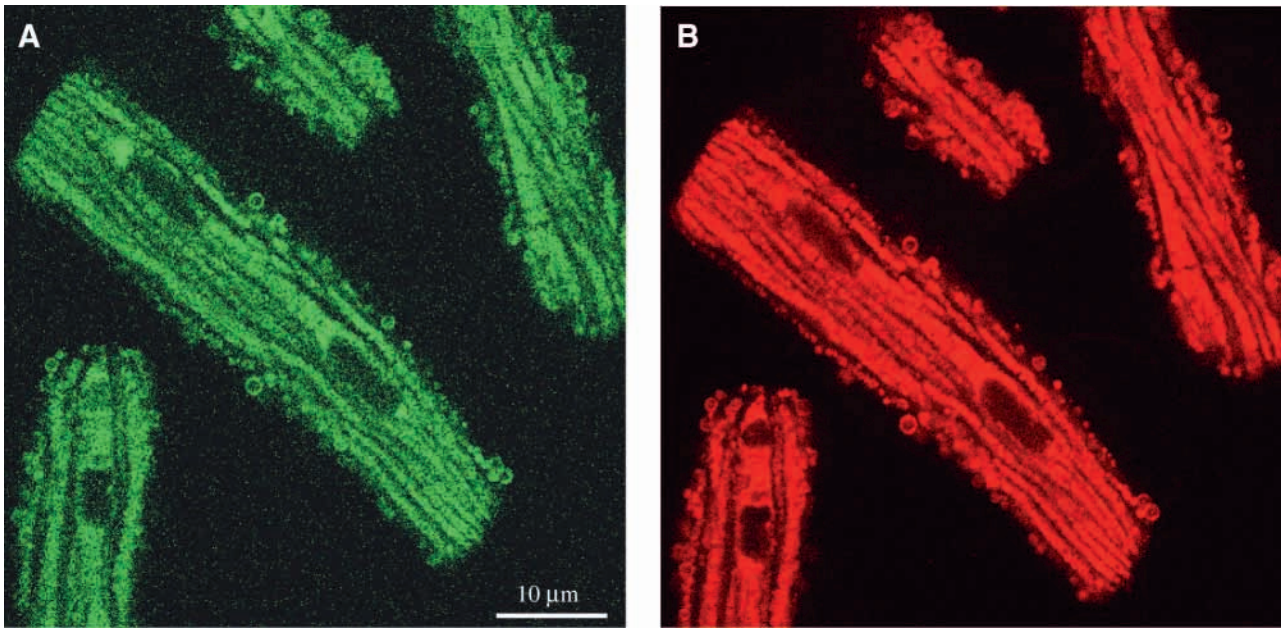


Fig. 1. Simultaneous imaging (co-localization) of mitochondrial flavoproteins (A) and calcium (B) in permeabilized cardiomyocytes loaded with Rhod-2. (A) Autofluorescence of mitochondrial flavoproteins in a fully oxidized state in the absence of mitochondrial substrates shows a regular arrangement of mitochondria in saponin-permeabilized cells. (B) Fluorescence of Rhod-2 trapped in mitochondria allows the localization and quantification of mitochondrial free calcium. Clear co-localization of flavoproteins (green fluorescence) and mitochondrial calcium (red fluorescence) can be seen.

At 21°C, pH 7 and an ionic strength of 0.175 mol $l^{-1}$, the total calcium concentrations required to obtain the free calcium concentrations of 0.1, 0.4, 1.0, 2.0 and 3.0 µmol $l^{-1}$ used in the experiments were 1.81, 4.71, 6.93, 8.22 and 8.76 mmol $l^{-1}$, respectively.

*Mathematical modeling of heterogeneous ADP diffusion inside cardiomyocytes*

In this study, we used a modified version of our original mathematical model of compartmentalized energy transfer (Aliev and Saks, 1997; Vendelin et al., 2000). To study the ADP diffusion only, the concentrations of creatine and phosphocreatine were assumed to be zero, corresponding to the experimental conditions without creatine. The reaction rates of all enzymes were reduced four times in comparison with the data of our earlier publication (Vendelin et al., 2000) to take into account the difference in temperature (25°C was used in the present study with skinned cardiac fibers instead of 37°C as used previously). The ATPase activity ($\dot{v}_{ATP}$) in skinned fibers is taken not to be periodic (due to non-contracting fibers) but to be stationary and dependent on the concentrations of MgATP and MgADP ([MgATP] and [MgADP], respectively), according to the equation:

$$v_{ATP} = \frac{V_{ATP}[MgATP]}{[MgATP] + K_{ATP}\{1 + ([MgADP]/K_{ADP})(1 + [Pi]/K_{Pi})\}}, \quad (2)$$

where $[P_i]$ is inorganic phosphate concentration, $K_{ATP}$, $K_{ADP}$ and $K_{Pi}$ are the dissociation constants for ATP, ADP and $P_i$, respectively, and $\dot{V}_{ATP}$ is the maximal rate of the ATPase reaction. Since $[P_i]$ was not changed in the present study but kept constant at 3 mmol $l^{-1}$, in calculations we used an apparent dissociation constant for ADP [$K'_{ADP}=K_{ADP}/(1+[P_i]/K_{Pi})$]. We assumed that $K_{ATP}$ and $K'_{ADP}$ were the same and are in the range of 100–300 µmol $l^{-1}$ (Yamashita et al., 1994). The ATPase activity was assumed to be distributed homogeneously in the myofibrillar compartment and cytoplasm.

In this version of the model, we took into account the geometry of skinned fiber and the boundary conditions imposed in experiments. The permeabilized cardiac cell was considered as a cylinder 20 µm in diameter (Figs 1, 2). Because of careful separation of fibers before permeabilization, the diameter of skinned cardiac muscle fibers was close to that of cardiomyocytes (Fig. 3). This assumption is in agreement with an observation that the apparent $K_m$ for exogenous ADP is equally very high for isolated cardiomyocytes and skinned cardiac fibers (Saks et al., 1991, 1993; Kay et al., 1997; see below). We assumed that the concentrations of the metabolites within the solution were uniform due to stirring during the experiments. Using this assumption and taking into account the small ratio of the diameter to the length of the fiber, we simulated the diffusion between the fiber and the solution only in one cross-section. The cross-section was populated with the mitochondria (diameter 1 µm). Mitochondria were distributed randomly in the cross-section to fill 25% of the fiber volume. The concentrations of the metabolites in the solution and the fiber were approximated in

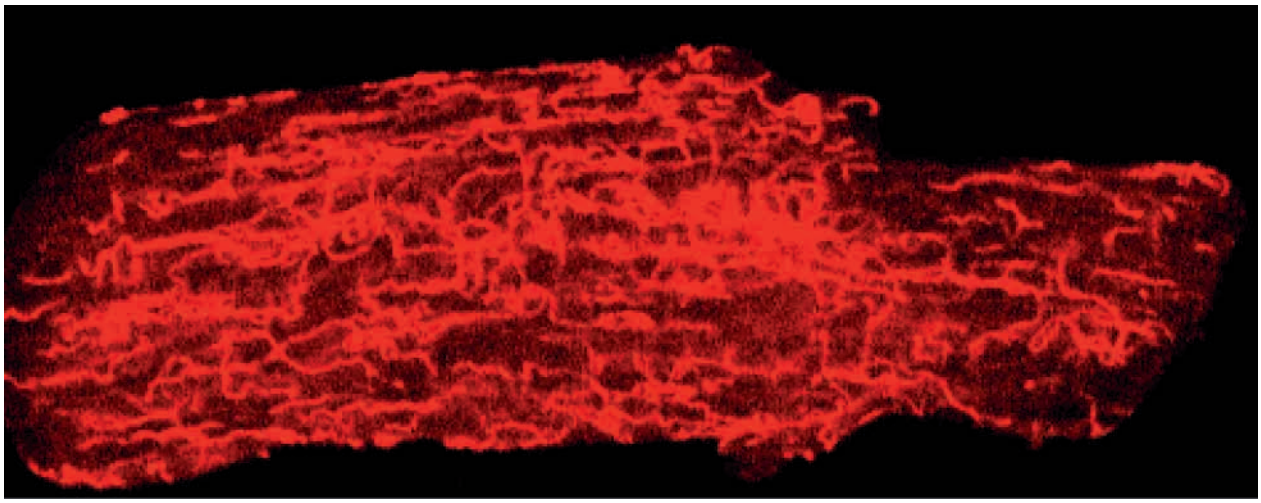

Fig. 2. Localization of cytoskeletal microtubular network in a selectively permeabilized cardiomyocyte. Imaging of microtubular network by monoclonal antibodies against tubulin demonstrates equal fluorescence over the entire cardiomyocyte, indicating complete accessibility to these tubulin antibodies. Cell size is the same as in Fig. 1.

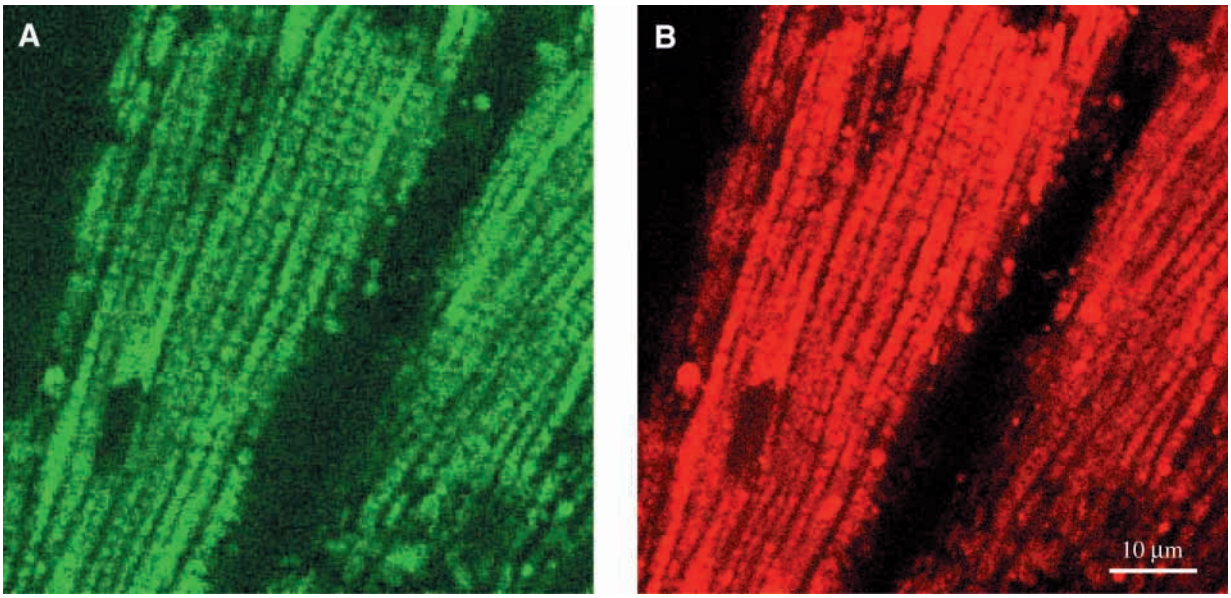


Fig. 3. Simultaneous imaging (co-localization) of mitochondrial flavoproteins (A) and calcium (B) in permeabilized myocardial fibers loaded with Rhod-2. (A) As in the case of isolated cells, autofluorescence of mitochondrial flavoproteins in a fully oxidized state in the absence of mitochondrial substrates shows a regular arrangement of mitochondria in saponin-permeabilized fibers. (B) Fluorescence of Rhod-2 trapped in mitochondria allows the localization and quantification of mitochondrial free calcium. As in cardiomyocytes (Fig. 1), clear co-localization of flavoproteins (green fluorescence) and mitochondrial calcium (red fluorescence) can be seen.

the following way. The relative volumes of fibers and surrounding solution were taken into account (the ratio was assumed to be 1:1000). Within the fiber, the concentration of the metabolites in myoplasm and myofibrils was approximated using the finite elements. The diffusion path of a metabolite was divided into the following three parts: (1) restricted diffusion from or into (for endogenous ADP) the solution through the cytoplasmic and myofibrillar space and into the vicinity of each mitochondria, with an apparent diffusion coefficient ($D_{app}$); (2) passive diffusion through the outer mitochondrial membrane; and (3) carrier-mediated exchanges from the intermembrane space into the mitochondrial matrix. In our simulations, the concentrations of the metabolites were computed at the nodal points of the elements. The flux of the metabolites between the mitochondrion and the myoplasmatic/myofibrillar compartment is determined by permeability of the outer membrane and by the gradients of metabolite concentration in the intermembrane space and on the finite element nodes lying on the boundary between the mitochondrion and myoplasmatic/myofibrillar compartment. The concentrations of the metabolites

Table 1. *Measured apparent $K_m$ for exogenous ADP in different permeabilized cell preparations, and diffusion distances from the medium into the center of cells ($R_{dif}$)*

| Preparation | Measured diameter (μm) | $R_{dif}$ (μm) | Apparent $K_m$ (ADP) (μmol $l^{-1}$) | Reference |
|---|---|---|---|---|
| Cardiomyocytes | 10–25 | 5–12.5 | – | Opie, 1998 |
| | – | – | 329±50* | Present study |
| | 16 | 8 | 250±38 | Saks et al., 1991 |
| | 20 | 10 | 200–250 | Kay et al., 1997 |
| 'Ghost' cardiomyocytes | 20 | 10 | 200–250 | Kay et al., 1997 |
| Skinned cardiac fibers | – | – | 297±35 | Saks et al., 1993 |
| | 20 | 10 | 300±23 | Saks et al., 2001 |
| | – | – | 300–400 | Seppet et al., 2001 |
| | – | – | 370±70 | Boudina et al., 2002 |
| | – | – | 234±24 | Liobikas et al., 2001 |
| | 22 | 11 | – | Menin et al., 2001 |
| | – | – | 334±48* | Present study |
| 'Ghost' cardiac fibers | 20 | 10 | 349±24 | Saks et al., 1993 |
| | – | – | 349±34* | Present study |
| Skinned cardiac fibers + creatine | – | – | 79±8 | Saks et al., 1991 |
| | – | – | 85±5 | Kuznetsov et al., 1996 |
| Rat heart mitochondria *in vitro* | ~1 | 0 | 17.6±1 | Saks et al., 1991 |

*Measured in this work for preparations similar to those described in Fig. 1. The diffusion distances are given to evaluate the rate of Brownian movement of ADP in water, if necessary (Saks et al., 2001).

(ADP, Pi and ATP) in the mitochondrial matrix were calculated from their concentrations in the intermembrane space and by the kinetics of adenine nucleotide and phosphate transport (Vendelin et al., 2000). Respiration rates were calculated as the functions of the metabolite concentrations in the mitochondrial matrix (Vendelin et al., 2000).

In simulations presented here, we added a description of the pyruvate kinase reaction rate ($\dot{v}_{PK}$; Saks et al., 1994). Homogenous distribution of PK was assumed in solution and in myofibrillar and cytoplasmatic compartments of the permeabilized fibers. In the model, the apparent diffusion coefficient of a metabolite in the myofibrillar and cytoplasmatic compartments ($D_{app}$=DF×$D_0$, where DF is a diffusion coefficient factor, and $D_0$ is a diffusion coefficient in the water or in the bulk water phase in cytoplasm) was varied by giving different values to DF: the degree of inhibition of mitochondrial respiration by the PK–PEP system at different PK activities was computed for two values of DF: DF=1, representing the Brownian movement in the water, and DF=$10^{-1.8}$, found from fitting the experimental data.

The complete model used in these calculations is available online at the following address: http://cens.ioc.ee/~markov/jexpbiol.2003/jexpbiol.model.pdf.

## Results

### *Confocal microscopic imaging of the cellular systems studied*

Figs 1–3 show the detailed characteristics of the permeabilized cardiomyocytes and skinned myocardial fibers in solution B with pCa=7.0, which corresponds to the resting state of the cell. Fig. 1 shows the confocal microscopic imaging, both by autofluorescence of flavoproteins (Fig. 1A) and intramitochondrial calcium (Fig. 1B), of mitochondria in isolated and permeabilized rat cardiomyocytes in solution B. The cardiomyocytes are relaxed and of rod-like shape, and, inside the cells, mitochondria are regularly arranged between myofibrils. Fig. 2 shows that the permeabilization process is complete and allows excellent immunofluorescence staining of the microtubular network in the cells. The network is intact, showing that the cytoskeleton of the cells is well preserved during the permeabilization procedure. An alternative, and more rapid and simple, technique for isolation of cardiomyocytes is to use the permeabilized ('skinned') muscle fibers (Fig. 3). This technique requires careful separation of muscle bundles into fibers, where the cardiac cells maintain their contacts with each other at intercalated discs (Veksler et al., 1987; Saks et al., 1998a; Fig. 3) but the fiber diameter is the same as that of cardiomyocytes (10–20 μm), and the diffusion distances (correspondingly, 5–10 μm) and diffusion kinetics for substrates and ADP are always the same as those of cardiomyocytes (Table 1). While isolation of cardiomyocytes requires the use of whole rat hearts and is rather time-consuming, the permeabilized fiber technique needs only a few milligrams of muscle tissue, which is crucial, for example, in human and clinical studies (Walsh et al., 2001; Kuznetsov et al., 1998). The two methods, however, are equally good for

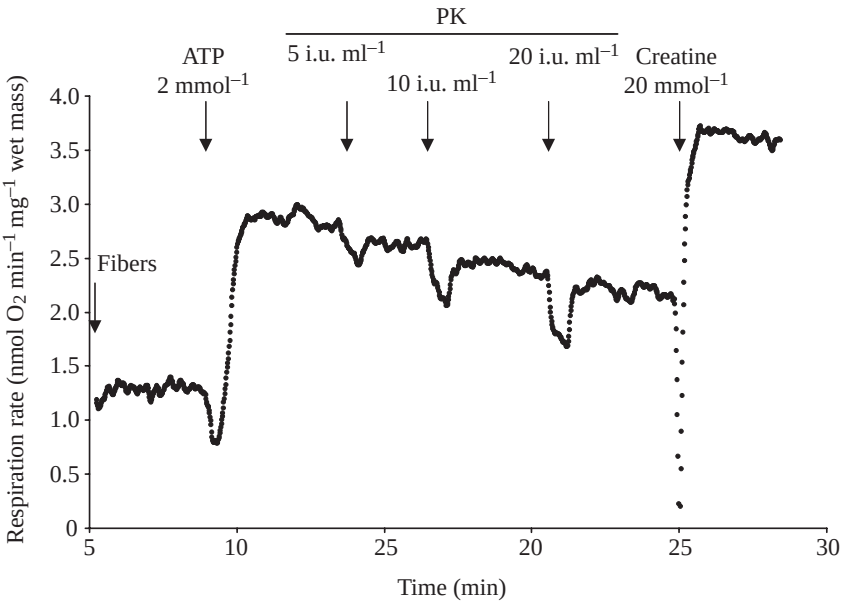


Fig. 4. Recordings of the respiration rate in permeabilized myocardial fibers activated by endogenous ADP production in MgATPase reactions. Traces show the rate of change of oxygen concentration in time in an oxygraph cell. Respiration rates were measured in the presence of 5 mmol $l^{-1}$ glutamate plus 2 mmol $l^{-1}$ malate, as described in Materials and methods. Addition of 2 mmol $l^{-1}$ ATP, and various final concentrations of pyruvate kinase (PK) in the presence of 2 mmol $l^{-1}$ phosphoenolpyruvate (PEP) in the medium are indicated. At the end of experiments, 20 mmol $l^{-1}$ creatine was added. Arrows show the time of addition. The results show some inhibitory effect of the competitive pyruvate kinase (PK)–PEP system for endogenous ADP on the respiration rate and a stimulatory effect of creatine, due to coupled creatine kinase reaction, in the presence of PK. Only minor inhibition of respiration by very high PK activity (20 i.u. $ml^{-1}$) demonstrates compartmentation and direct channeling of endogenous ADP. These effects of direct channeling are increased after activation of mitochondrial creatine kinase.

studying the whole population of mitochondria inside the cell in their natural surroundings.

*Respiratory characteristics of permeabilized cell systems*

The rate of oxidative phosphorylation (mitochondrial ATP production) is regulated by ADP due to the respiratory control phenomenon (Chance and Williams, 1956). The affinity of oxidative phosphorylation for ADP is quantitatively characterized by an apparent $K_m$ for ADP. For isolated mitochondria in the homogenous suspension, the value of this constant for ADP in the medium (exogenous ADP) is very low, 10–20 μmol $l^{-1}$, due to the high permeability of the outer mitochondrial membrane (Klingenberg, 1970) and high affinity of adenine nucleotide translocator for this substrate (Vignais, 1976). However, when mitochondria are studied in the permeabilized cells *in situ*, the results are very different (Saks et al., 1998a).

Table 1 summarises the measured affinities of mitochondria for exogenous ADP in different preparations before (intact permeabilized cells) and after (ghost cells or fibers) extraction of myosin. In spite of the very small diffusion distances (mean=10 μm) from the medium into the core of the cells (Figs 1–3), in all cases the affinities are very low compared with the very high values of apparent $K_m$ for exogenous ADP (300–400 μmol $l^{-1}$). An important observation shown in Table 1 is that activation of the mitochondrial creatine kinase (miCK) reaction decreases the value of apparent $K_m$ for exogenous ADP. This is due to functional coupling of the miCK reaction to the oxidative phosphorylation *via* the adenine nucleotide translocator (Barbour et al., 1984; Joubert et al., 2002; Saks et al., 1975, 1994, 1995; Wallimann et al., 1992; Wyss and Kaddurah-Daouk, 2000), which leads to increased local turnover of adenine nucleotides in mitochondria, effective aerobic phosphocreatine production and metabolic stability of the heart (Garlid, 2001; Kay et al., 2000; Saks et al., 1995). This emphasizes the role of miCK in regulation of mitochondrial respiration in muscle cells (Joubert et al., 2002; Kay et al., 2000; Saks et al., 2001; Walsh et al., 2001).

Further evidence for this kind of local control of respiration by miCK is provided in Fig. 4, which shows the oxygraph recordings of mitochondrial respiration in skinned cardiac fibers when ADP was produced endogenously in the cellular MgATPase reactions in the presence of 2 mmol $l^{-1}$ MgATP. Endogenous ADP production activates respiration several times. Subsequent addition of a system competing with mitochondria for ADP (Gellerich and Saks, 1982), consisting of pyruvate kinase (PK) in high concentrations and phosphoenolpyruvate (PEP), reduced the respiration rate, but not by more than 40%. Addition of creatine increased the respiration rate to its maximal value observed in State 3. This is again due to activation of local production of ADP by miCK in the mitochondrial intermembrane space, and this locally produced ADP is totally inaccessible for exogenous PK but is channeled to the adenine nucleotide translocator and transported into the mitochondrial matrix (see above).

Explanation of these experimental data and of the low efficiency of inhibition of respiration by exogenous PK can be found by using the mathematical model of ADP diffusion and energy transfer inside the cells (see Materials and methods). Fig. 5 shows the results of calculations of the respiration rate for two different situations. First, the diffusion coefficient, $D$, for ADP and ATP was taken to be equal to that in the cellular bulk water phase, $D_0$=145 $\mu m^{-2}$ $s^{-1}$ (Aliev and Saks, 1997). In this case, because of the small diffusion distance and the high rate of diffusion (high value of $D$), ATP and ADP are rapidly

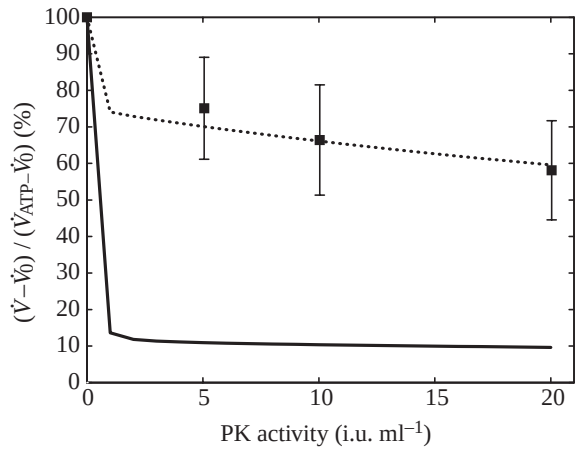


Fig. 5. The computer modeling of data shown in Fig. 4 on the reduction of respiration rate of mitochondria *in situ* in permeabilized cardiac cells dependent on endogenous ADP (in the presence of 2 mmol l$^{-1}$ MgATP) by increasing pyruvate kinase (PK) activity for two different systems. $\dot{V}$, respiration rate under given conditions; $\dot{V}_0$, respiration rate before addition of ATP; $\dot{V}_{ATP}$, respiration rate in the presence of 2 mmol l$^{-1}$ ATP. Solid line: diffusion constant of ADP was taken as $D_0$ (characteristic for Brownian movement in water phase). Broken line: apparent diffusion coefficient was changed to fit the experimental data (separate points show the mean values ± S.D. of respiration rate for given pyruvate kinase activity). Good correlation between simulations and the measurements was obtained for DF=$10^{-1.8}$.

exchanged between extra- and intracellular spaces, and ADP produced endogenously in the cellular MgATPase reactions is very rapidly consumed by PK (solid line in Fig. 5). The result is that respiration is effectively suppressed already in the presence of PK at activities below 5 i.u. ml$^{-1}$ in the medium (solid line in Fig. 5). These data are in agreement with our previous conclusions that the Brownian movement of ADP in water phase across 10 μm is much faster than its metabolic turnover in heart mitochondria (Saks et al., 2001).

However, the curve for $D_0$ is much lower than the experimental dependence (Fig. 5, experimental points). To fit the experimental results described in Figs 4 and 5, we decreased the mean, apparent diffusion coefficient ($D_{app}$=DF×$D_0$), inside the cells, assuming that the high degree of intracellular structural organization (see Figs 1–3) may restrict the diffusion of adenine nucleotides (Saks et al., 2001). A good fit between the results of the modeling and the experimental data was observed when the DF approached the value of $10^{-2}$ (Fig. 5). This means that the intracellular diffusion of ADP (and ATP) is likely to be very heterogeneous and strongly restricted in some areas inside the cells. Probably, this occurs both at or near the outer mitochondrial membrane and between the ICEUs (Aliev and Saks, 1997; Saks et al., 1994, 2001).

It is also known that the high values of apparent $K_m$ for exogenous ADP are significantly decreased from 300–350 μmol l$^{-1}$ to 40–70 μmol l$^{-1}$ by selective proteolysis (Kuznetsov et al., 1996; Saks et al., 2001). Treatment of permeabilized cardiomyocytes for a short time with 1 μmol l$^{-1}$ trypsin also results in rapid disorganisation of the regular arrangement of mitochondria in cardiomyocytes and a collapse in the microtubular network (Appaix et al., 2003). Thus, evidently under these conditions, the specific structure of ICEUs is lost and the local intracellular restrictions for ADP diffusion are eliminated. This may well explain the decrease in apparent $K_m$ for exogenous ADP. In addition, we have shown previously that, after similar proteolytic treatment, the endogenous ADP becomes more accessible for the exogenous PK reaction (Saks et al., 2001).

The hypothesis of the heterogeneity of intracellular diffusion of ADP related to the structure of ICEUs is consistent with the new surprising findings described below.

### *The apparent link between sarcomere length and kinetic parameters of respiration regulation*

The results described in Figs 6–8 show a new interesting phenomenon – an apparent link between sarcomere length and the affinity of mitochondria for exogenous ADP, measured as an apparent $K_m$ for this substrate in regulation of mitochondrial respiration in the permeabilized cells *in situ*. This phenomenon was observed when the kinetics of regulation of respiration by ADP were studied at different free calcium concentrations in two systems: permeabilized cardiac muscle fibers and permeabilized 'ghost' fibers after extraction of myosin. The free calcium concentration was increased from 0.1 μmol l$^{-1}$ to 3 μmol l$^{-1}$, which corresponds to the physiological range of concentrations (Bers, 2001). Fig. 6 shows that, in the presence of ATP (or respiratory substrates and ADP), an increase of free $Ca^{2+}$ concentration to 3 μmol l$^{-1}$ results in strong contraction of sarcomeres and shortening of fiber length in intact permeabilized cardiac fibers. If the fibers are not fixed, intermyofibrillar mitochondria seem to fuse as a result of being pressed together; if the fibers are fixed in flexiperm and contract isometrically, one observes the appearance of the empty areas and of a rather long distance between mitochondria. In both cases, the structure of the cell and the structure of ICEUs are deformed.

Extraction of myosin prevents these $Ca^{2+}$-induced structural changes (Fig. 7). The removal of a significant proportion of myosin decreased the total MgATPase activity of fibers (measured in the presence of 3 mmol l$^{-1}$ MgATP) from approximately 4.5–5.0 nmol/min mg$^{-1}$ wet mass (initial mass) to 0.9–1.0 nmol/min mg$^{-1}$ wet mass. In ghost fibers, a very regular arrangement of mitochondria with a precise, parallel fixation in the *y*–*z* plane of cells was observed (direction of fiber orientation perpendicular to the *x*-axis), giving the impression of a striated pattern for the intracellular distribution of mitochondria. In these ghost fibers, the regular distance between mitochondria, corresponding to sarcomere length, is not changed with alteration of calcium concentration (Fig. 7). Thus, there is no deformation of the internal, modified structure of the ICEUs in the cell.

Fig. 8 shows that, surprisingly, the apparent $K_m$ for

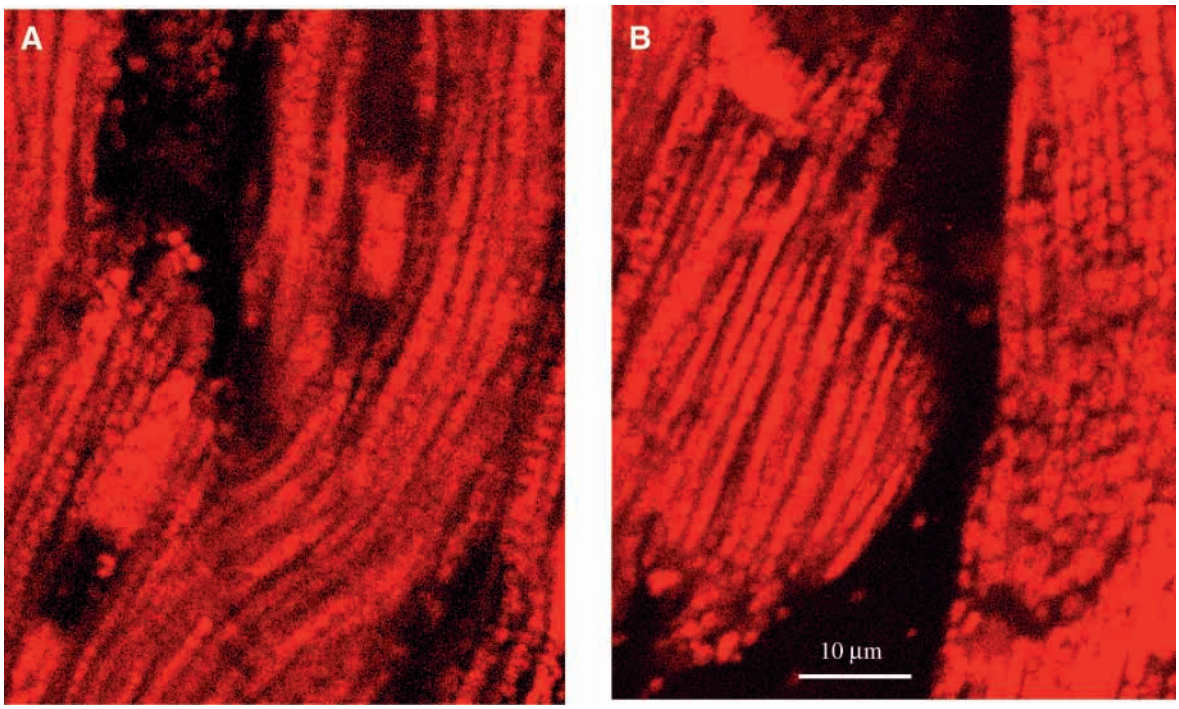


Fig. 6. Imaging of mitochondria in permeabilized myocardial fibers by the membrane-potential-sensitive probe teramethylrhodamine ethyl ether (TMRE). (A) Fibers in the presence of 2 mmol $l^{-1}$ ATP, 2 mmol $l^{-1}$ malate and 5 mmol $l^{-1}$ glutamate (concentration of free $Ca^{2+}$ in Ca-EGTA buffer: 0.1 µmol $l^{-1}$). (B) The same fibers after addition of calcium chloride (final concentration of free $Ca^{2+}$ in Ca-EGTA buffer: 1.0 µmol $l^{-1}$). The left fiber in a flexiperm chamber was not fixed, while the right (longer) fiber was fixed by its ends. In A, both fibers are relaxed. In B, the left fiber is contracted, while the right fiber, which is contracting almost isometrically, shows significant structural changes due to sarcomere contraction. Note the empty spaces between mitochondria.

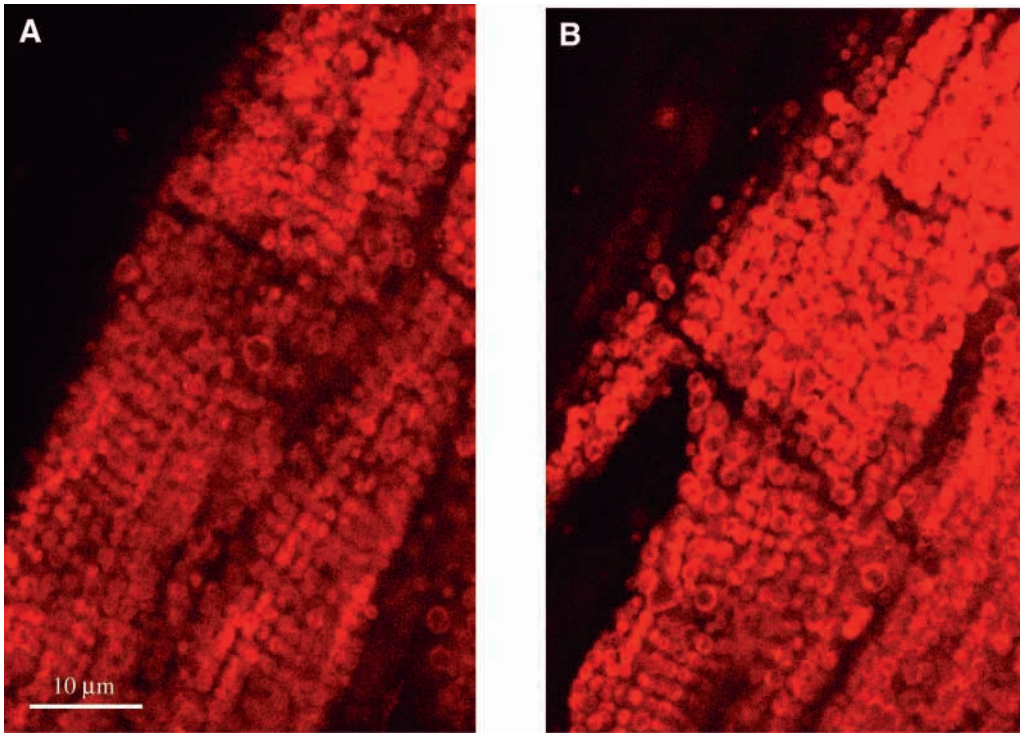


Fig. 7. Imaging of mitochondria in permeabilized myocardial fibers after extraction of myosin (ghost fibers) by membrane-potential-sensitive probe tera-methylrhodamine ethyl ether (TMRE). (A) Ghost fibers in the presence of 2 mmol $l^{-1}$ ATP, 2 mmol $l^{-1}$ malate and 5 mmol $l^{-1}$ glutamate (concentration of free $Ca^{2+}$ in Ca-EGTA buffer: 0.1 µmol $l^{-1}$). (B) The same ghost fibers after addition of calcium chloride (final concentration of free $Ca^{2+}$ in Ca-EGTA buffer: 1.0 µmol $l^{-1}$). No structural changes were seen. The same result was obtained for a free $Ca^{2+}$ concentration of 3 µmol $l^{-1}$.

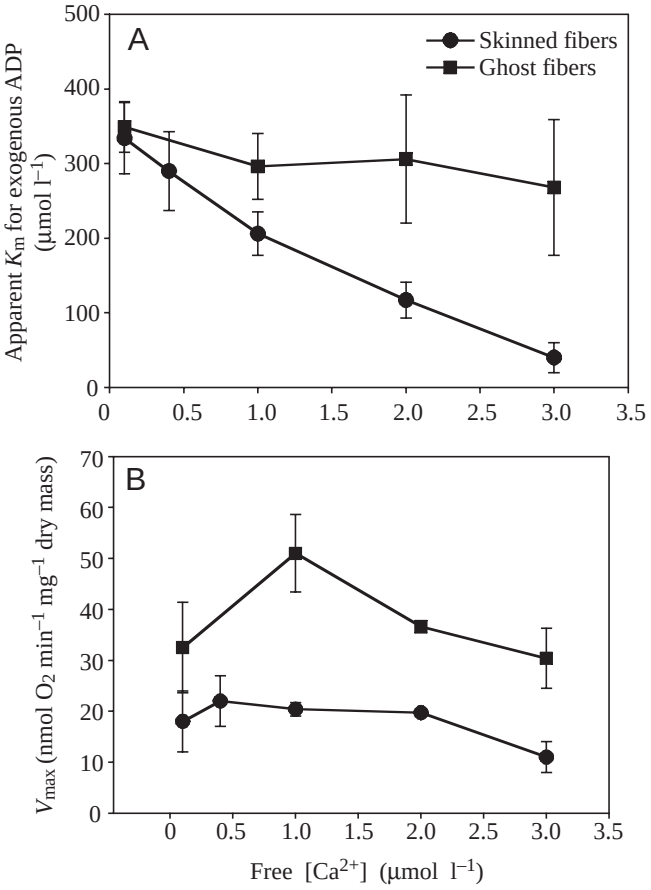


Fig. 8. Effect of different free $Ca^{2+}$ concentrations on parameters of ADP kinetics of mitochondrial respiration in permeabilized myocardial fibers and in myosin-extracted (ghost) fibers. (A) Effect of $Ca^{2+}$ on apparent $K_m$ for ADP. A dramatic decline in the apparent $K_m$ for ADP was observed in control fibers. By contrast, no changes in apparent $K_m$ for ADP can be seen in ghost fibers. (B) Effect of different free $Ca^{2+}$ concentrations on $V_{max}$.

exogenous ADP in regulation of mitochondrial respiration in intact permeabilized fibers decreases from 350 μmol l$^{-1}$ to 30 μmol l$^{-1}$ with elevation of the free calcium concentration to 3 μmol l$^{-1}$ and deformation of the cell structure (Fig. 8A). A decrease in the $V_{max}$ of respiration was also observed (Fig. 8B). None of these changes are observed in ghost fibers. In spite of removal of myosin and a 5-fold decrease in the overall MgATPase activity, the apparent $K_m$ for exogenous ADP (349±34 μmol l$^{-1}$) is initially (at 0.1 μmol l$^{-1}$ free calcium concentration) equal to that of intact permeabilized fibers and always stays above 250 μmol l$^{-1}$, even when free $Ca^{2+}$ concentration is increased to 3 μmol l$^{-1}$ (Fig. 8A). $V_{max}$ does not change either with alteration of the free $Ca^{2+}$ concentration (Fig. 8B; in comparison with intact permeabilized fibers, $V_{max}$ is elevated in ghost fibers due to extraction of a large proportion of the protein, i.e. myosin). Stability of all mitochondrial functions in ghost fibers shows that changes in the free $Ca^{2+}$ concentration in the range used does not alter the mitochondria, which might result from a mechanism of the permeability transition pore (PTP) opening (Lemasters et al., 1998).

An important conclusion from these data is that their seems to be a direct structural and functional link between sarcomere structure and mitochondrial function, which is in agreement with the concept of ICEUs.

## Discussion

The results of this study conform to the hypothesis of the existence of structural and functional complexes [intracellular energetic units (ICEUs)] between mitochondria, sarcoplasmic reticulum and myofibrils in the cardiac cells (Saks et al., 2001; Seppet et al., 2001; Kaasik et al., 2001). They show that structural connections between mitochondria and sarcomeres (and probably sarcoplasmic reticulum) inside ICEUs are so strong that there exists a direct link between sarcomere length and regulation of mitochondrial function. Organization of mitochondria into ICEUs results in the heterogeneity of the intracellular diffusion of ADP (and ATP), a phenomenon which is in agreement with the general theories of the compartmentation of adenine nucleotides in the cardiac cells (Gudbjarnason et al., 1970; Saks et al., 1995, 1998b; Weiss and Korge, 2001). This conclusion is in good agreement with *in vivo* $^{31}$P-NMR pulsed-field gradient data showing heterogeneity of intracellular diffusion of phosphorus metabolites in red and white skeletal muscles from fish (Kinsey et al., 1999) and in skeletal muscle of rat (de Graaf et al., 2000). One of the consequences of the heterogeneity of ADP and ATP diffusion is the very high values of apparent $K_m$ for exogenous ADP in permeabilized cells and differences in the kinetics of respiration regulation by exogenous and endogenous ADP (Seppet et al., 2001). Metabolic consequences of this structural and functional organisation of cardiac muscle cells are that mitochondrial function, and thus cell respiration and free energy transductions, is regulated *in vivo* by channeling of substrates, such as ADP and ATP, in the energy-transfer and signalling creatine kinase and adenylate kinase networks within these functional complexes. This is due to tight functional coupling of enzymes and protein–protein interactions (Dzeja et al., 1998, 1999; Saks et al., 1998b; Walsh et al., 2001; Weiss and Korge, 2001), which may also include the rather tight control of the outer mitochondrial membrane (Saks et al., 1995). Thus, the metabolic regulation in cardiac cells is an organised process, leaving little space for random events that usually determine the kinetics of enzyme reactions in diluted homogenous solutions and, as a consequence, excluding the equilibrium kinetics of respiration regulation usually accepted in the literature. Instead, the regulation of respiration and cellular energetics in general are better understood as a steady state of channelled metabolic fluxes. Fig. 9 illustrates this highly organized functional unit, the ICEU, as a basic pattern of metabolic regulation in cardiac cells.

It is well known that patterns of metabolic regulation are very different in different muscle cells (Hochachka and

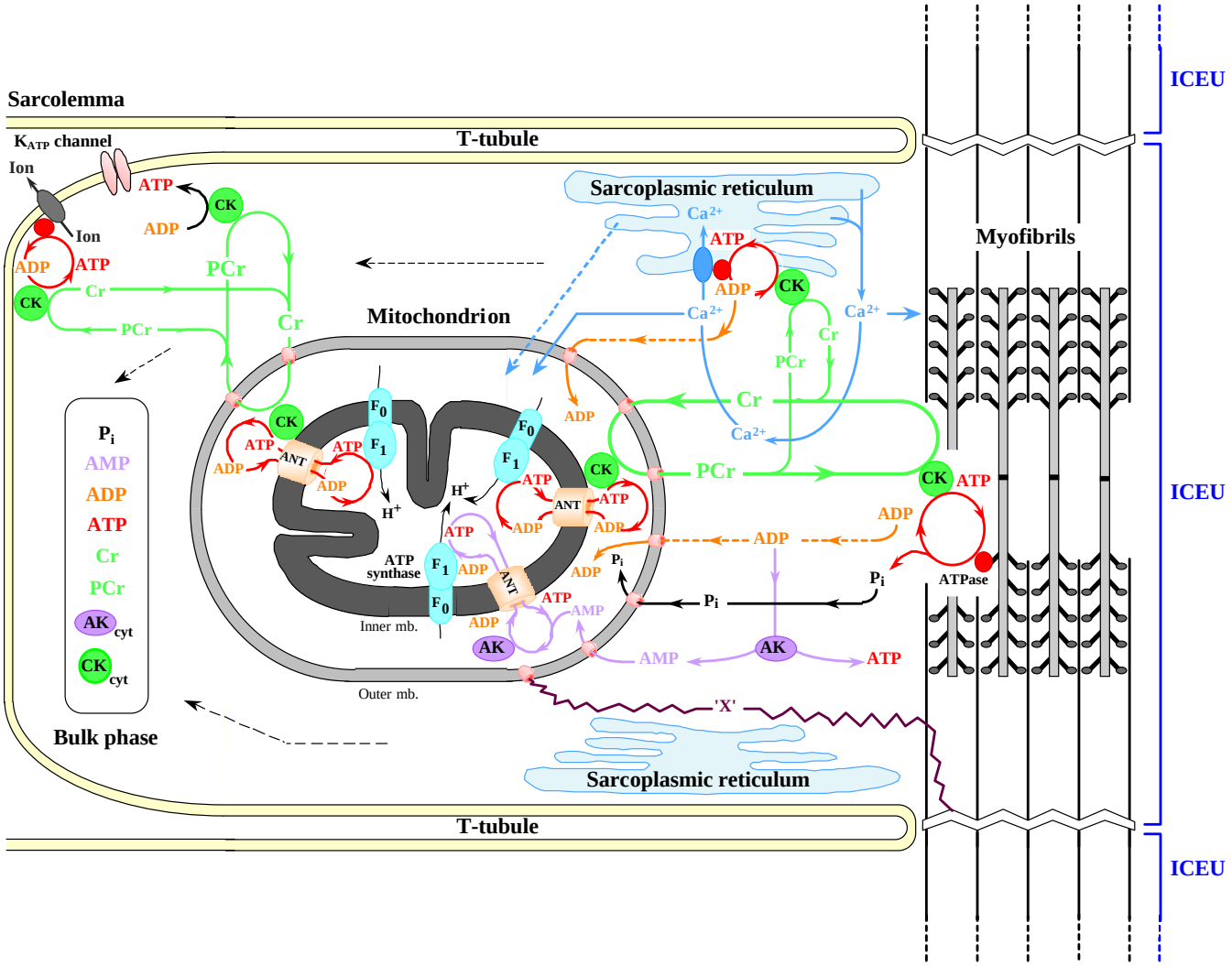


Fig. 9. Scheme illustrating the functional intracellular energetic units (ICEUs) in the cardiac cell. By interaction with cytoskeletal elements, the mitochondria and sarcoplasmic reticulum (SR) are precisely fixed with respect to the structure of the sarcomere of the myofibrils between two Z-lines and, correspondingly, between two T-tubules. Calcium is released from the SR into the space in the ICEU in the vicinity of the mitochondria and sarcomeres to activate contraction and mitochondrial dehydrogenases. Adenine nucleotides within the ICEU do not equilibrate rapidly with adenine nucleotides in the bulk water phase. The mitochondria, SR and MgATPase of myofibrils and ATP-sensitive systems in the sarcolemma are interconnected by metabolic channeling of reaction intermediates and energy transfer within the ICEU by the creatine kinase (CK)–phosphocreatine (PCr) and adenylate kinase (AK) systems. $CK_{cyt}$ and $AK_{cyt}$ represent the CK and AK in the cytoplasmic space. $F_0F_1$ is the mitochondrial ATPase synthase complex. The protein factors (still unknown and marked as 'X'), most probably connected to cytoskeleton, fix the position of mitochondria and probably also control the permeabilty of the VDAC channels to ADP and ATP. Adenine nucleotides within the ICEU and bulk water phase may be connected by some more rapidly diffusing metabolites than creatine (Cr)–PCr. Synchronization of functioning of ICEUs within the cell may occur by the same metabolites, for example, inorganic phosphate ($P_i$) or PCr, and/or synchronized release of calcium during the excitation–contraction coupling process. Adapted from Saks et al., 2001.

McClelland, 1997). In the heart, oxygen consumption rate increases linearly (more than 10 times compared with the resting state) with the increase in workload without changes in high-energy phosphate, notably phosphocreatine levels (Williamson et al., 1976; Balaban et al., 1986). Thus, this is the system of highest efficiency of feedback regulation. In skeletal muscle, on the other hand, the phosphocreatine level decreases rapidly, even during short periods of work, and the decline is faster (correspondingly, post-exercise recovery is slower) in the fast-twitch glycolytic muscles than in the oxidative slow-twitch skeletal muscle (Kushmerick et al., 1992). The mitochondrial content and its intracellular arrangement are also remarkably different: fast-twitch glycolytic muscles have a very low number of mitochondria, which are localized close to the T–tubule systems near the Z-line of sarcomeres (Ogata and Yamasaki, 1997), while in slow-twitch oxidative muscles, and especially in cardiac muscle, mitochondria are localized in the intermyofibrillar space at the

level of the A-band of sarcomeres (Duchen, 1999; Boudina et al., 2002). These structural differences are paralleled by differences in functional characteristics, in particular in the apparent $K_m$ for exogenous ADP (Kuznetsov et al., 1996; Burelle and Hochachka, 2002). Thus, both intracellular arrangement and regulation of mitochondrial respiration are tissue specific.

This also seems to be true for mitochondrial–cytoskeletal interactions in general. In many types of cells, one sometimes observes rather vigorous movement of mitochondria due to their interaction with cytoskeletal elements, such as the microtubular network and actin microfilaments (Bereiter-Hahn and Voth, 1994; Leterrier et al., 1994; Margineantu et al., 2000; Rizzutto et al., 1998; Yaffe, 1999). In some cases, the molecular bases behind the organellar movement of microtubules are motor proteins, kinesin and cytoplasmic dynein, which bind microtubules and transduce chemical energy of ATP into mechanical work of mitochondrial movement along microtubules (Yaffe, 1999). One may think that, in cardiac cells, the mitochondria have arrived at their proper, fixed position inside functional complexes with sarcomeres and sarcoplasmic reticulum (ICEUs) to achieve the most effective regulation of cellular energetics. Indeed, during cardiac muscle development, intracellular distribution of mitochondria changes from a chaotic one in the early postnatal period to a very regular arrangement in the adult muscle (Tiivel et al., 2000). Since interaction with cytoskeleton is mediated by proteins associated with the outer mitochondrial membrane (Leterrier et al., 1994; Smirnova et al., 1998; Yaffe, 1999), it is easily feasible that these proteins also control the permeability of the voltage-dependent anion (VDAC) channels, of the outer mitochondrial membrane (Colombini, 1994) to adenine nucleotides. However, while the collapse of the microtubular network (Appaix et al., 2003) during short proteolysis coincides with disorganisation of the regular arrangement of mitochondria in cardiac cells and an increase in the apparent affinity for exogenous ADP in regulation of respiration as a result of elimination of local restrictions of diffusion, it is not clear if only (or if at all) the microtubular network participates in distribution of mitochondria in the cells and which type of cytolinker proteins is associated with the mitochondrial surface to fix them precisely inside the cells. These questions are exciting topics for further research.

The data reported in this work and conforming to the existence of ICEUs (Fig. 9) in the cardiac cells as a basic pattern of organisation of energy metabolism are in complete agreement with the recent evidence that mitochondria are morphologically and functionally heterogenous within the cells (Collins et al., 2002).

The strong effect of sarcomere contraction on the apparent $K_m$ for exogenous ADP observed in this work (Fig. 8) shows that structural connections between mitochondria and sarcomeres inside ICEUs are very significant. One of the possible explanations of this surprising phenomenon is that sarcomere contraction results in deformation of the mitochondrial outer membrane and opening of the VDAC pores to adenine nucleotides. Another possibility is that significant shortening of sarcomere length changes the structure of the ICEUs in general and makes the diffusion of exogenous ADP to mitochondria inside the cells easier. The observation made in this work is in good agreement with the data by Nozaki et al. (2001), who observed that in rat ventricular papillary muscle the mitochondrial length changes according to changes in sarcomere length during the transition from normoxia to hypoxia. Nevertheless, it is too early to speculate about the physiological significance of this observation. Understanding this phenomenon needs new experimental investigations.

This work was supported by INSERM, France and by Estonian Science Foundation grants (N° 4704, 4928, 4930). Skilful participation of Jose Olivares, Laurence Kay and Marina Panchishkina, University of Joseph Fourier, Grenoble, France and Maire Peitel, Tallinn in the experiments is gratefully acknowledged.

## References

**Aliev, M. K. and Saks, V. A.** (1997). Compartmentalised energy transfer in cardiomyocytes. Use of mathematical modeling for analysis of *in vivo* regulation of respiration. *Biophys. J.* **73**, 428-445.

**Anflous K., Armstrong, D. D. and Craigen, W. J.** (2001). Altered mitochondrial sensitivity for ADP and maintenance of creatine-stimulated respiration in oxidative striated muscles from VDAC1-deficient mice. *J. Biol. Chem.* **276**, 1954-1960.

**Appaix, F., Kuznetsov, A., Usson, Y., Kay, L., Andrienko, T., Olivares, J., Kaambre, T., Sikk, P., Margreiter, R. and Saks, V.** (2003). Possible role of cytoskeleton in intracellular arrangement and regulation of mitochondria. *Exp. Physiol.* **88**, 175-190.

**Balaban, R. S., Kantor, H. L., Katz, L. A. and Briggs, R. W.** (1986). Relation between work and phosphate metabolite in the *in vivo* paced mammalian heart. *Science* **232**, 1121-1123.

**Barbour, R. L., Ribaudo, J. and Chan, S. H. P.** (1984). Effect of creatine kinase activity on mitochondrial ADP/ATP transport. Evidence for functional interaction. *J. Biol. Chem.* **259**, 8246-8251.

**Bereiter-Hahn, J. and Voth, M.** (1994). Dynamics of mitochondria in living cells: shape changes, dislocations, fusion and fission of mitochondria. *Microsc. Res. Tech.* **27**, 198-219.

**Bers, D.** (2001). *Excitation–contraction Coupling and Cardiac Contraction*. Dordrecht: Kluwer Academic Publishers.

**Boudina, S., Laclau, M. N., Tariosse, L., Daret, D., Gouverneur, G., Boron-Adele, S., Saks, V. A. and Dos Santos, P.** (2002). Alteration of mitochondrial function in a model of chronic ischemia *in vivo* in rat heart. *Am. J. Physiol.* **282**, H821-H831.

**Braun, U., Paju, K., Eimre, M., Seppet, E., Orlova, E., Kadaja, L., Trumbeckaite, S., Gellerich, F., Zierz, S., Jockusch, H. and Seppet, E.** (2001). Lack of dystrophin is associated with altered integration of the mitochondria and ATPases in slow-twitch muscle cells of MDX mice. *Biochim. Biophys. Acta* **1505**, 258-270.

**Burelle, Y. and Hochachka, P. W.** (2002). Endurance training induces muscle-specific changes in mitochondrial function in skinned muscle fibers. *J. Appl. Physiol.* **92**, 2429-2438.

**Chance, B. and Williams, G. R.** (1956). The respiratory chain and oxidative phosphorylation. *Adv. Enzymol.* **17**, 65-134.

**Colombini, M.** (1994). Anion channels in the mitochondrial outer membrane. *Curr. Top. Membr.* **42**, 73-101.

**Collins, T. J., Berridge, M. J., Lipp, P. and Bootman, M. D.** (2002). Mitochondria are morphologically and functionally heterogenous within cells. *EMBO J.* **21**, 1616-1627.

**de Graaf, R. A., Van Kranenburg, A. and Nicolay, K.** (2000). *In vivo* $^{31}$P-NMR spectroscopy of ATP and phosphocreatine in rat skeletal muscle. *Biophys. J.* **78**, 1657-1664.

**Dos Santos, P., Kowaltowski, A. J., Laclau, M., Subramanian, S., Paucek,**

**P., Boudina, S., Thambo, J. B., Tariosse, L. and Garlid, K.** (2002). Mechanisms by which opening the mitochondrial ATP- sensitive K(+) channel protects the ischemic heart. *Am. J. Physiol*. 283, H284-H295.

**Duchen, M.** (1999). Contributions of mitochondria to animal physiology: from homeostatic sensor to calcium signalling and death. *J. Physiol*. **516**, 1-17.

**Dzeja, P. P., Zeleznikar, R. J. and Goldberg, N. D.** (1998). Adenylate kinase: kinetic behaviour in intact cells indicates it is integral to multiple cellular processes. *Mol. Cell. Biochem.* **184**, 169-182.

**Dzeja, P. P., Vitkevicius, K. T., Redfield, M. M., Burnett, J. C. and Terzik, A.** (1999). Adenylate-kinase catalyzed phosphotransfer in the myocardium: increased contribution in heart failure. *Circ. Res*. **84**, 1137-1143.

**Fabiato, A. and Fabiato, F.** (1979). Calculator programs for computing the composition of the solutions containing multiple metals and ligands used for experiments in skinned muscle cells. *J. Physiol*. **75**, 463-505.

**Fontaine, E. M., Keriel, C., Lantuejoul, S., Rigoulet, M., Leverve, X. M. and Saks, V. A.** (1995). Cytoplasmic cellular structures control permeability of outer mitochondrial membrane for ADP and oxidative phosphorylation in rat liver cells. *Biochem. Biophys. Res. Commun.* **213**, 138-146.

**Garlid, K.** (2001). Physiology of mitochondria. In *Cell Physiology Sourcebook. A Molecular Approach* (ed. N. Sperelakis), pp. 139-151. New York, Boston: Academic Press.

**Gellerich, F. and Saks, V. A.** (1982). Control of heart mitochondrial oxygen consumption by creatine kinase: the importance of enzyme localization. *Biochem. Biophys. Res. Commun*. **105**, 1473-1481.

**Godt, R. E. and Maughan, D. W.** (1988). On the composition of the cytosol of relaxed skeletal muscle of the frog. *Am. J. Physiol.* **254**, C591-C604.

**Gudbjarnason, S., Mathes, P. and Raven, K. G.** (1970). Functional compartmentation of ATP and creatine phosphate in heart muscle. *J. Mol. Cell. Cardiol* **1**, 325-339.

**Hochachka, P. W. and McClelland, G. B.** (1997). Cellular metabolic homeostasis during large-scale change in ATP turnover rates in muscles. *J. Exp. Biol.* **200**, 381-386.

**Joubert, F., Mazet, J. L., Mateo, P. and Joubert, J. A.** (2002). $^{31}$P NMR detection of subcellular creatine kinase fluxes in the perfused rat heart: contractility modifies energy transfer pathways. *J. Biol. Chem*. **277**, 18469-18476.

**Kaasik, A., Veksler, V., Boehm, E., Novotova, M., Minajeva, A. and Ventura-Clapier, R.** (2001). Energetic crosstalk between organelles. Architectural integration of energy production and utilization. *Circ Res*. **89**, 153-159.

**Kay, L., Li, Z., Fontaine, E., Leverve, X., Olivares, J., Tranqui, L., Tiivel, T., Sikk, P., Kaambre, T., Samuel, J. L., Rappaport, L., Paulin, D. and Saks, V. A.** (1997). Study of functional significance of mitochondrial–cytoskeletal interactions. *In vivo* regulation of respiration in cardiac and skeletal muscle cells of desmin-deficient transgenic mice. *Biochim. Biophys. Acta* **1322**, 41-59.

**Kay, L., Nicolay, K., Wieringa, B., Saks, V. and Wallimann, T.** (2000). Direct evidence of the control of mitochondrial respiration by mitochondrial creatine kinase in muscle cells *in situ*. *J. Biol. Chem*. **275**, 6937-6944.

**Kinsey, S. T., Locke, B. R., Benke, B. and Moerland, T. S.** (1999). Diffusional anisotropy is induced by subcellular barriers in skeletal muscle. *NMR Biomed*. **12**, 1-7.

**Klingenberg, M.** (1970). Mitochondrial metabolite transport. *FEBS Lett.* **6**, 145-154.

**Kummel, L.** (1988). Ca,MgATPase activity of permeabilized rat heart cells and its functional coupling to oxidative phosphorylation in the cells. *Cardiovasc. Res.* **22**, 359-367.

**Kushmerick, M. J., Meyer, R. A. and Brown, T. B.** (1992). Regulation of oxygen consumption in fast and slow-twitch muscle. *Am. J. Physiol.* **263**, C598-C606.

**Kuznetsov, A. V., Tiivel, T., Sikk, P., Käämbre, T., Kay, L., Daneshrad, Z., Rossi, A., Kadaja, L., Peet, N., Seppet, E. and Saks, V. A.** (1996). Striking difference between slow and fast twitch muscles in the kinetics of regulation of respiration by ADP in the cells in vivo. *Eur. J. Biochem.* **241**, 909-915.

**Kuznetsov, A. V., Mayboroda, O., Kunz, D., Winkler, K., Schubert, W. and Kunz, W. S.** (1998). Functional imaging of mitochondria in saponin-permeabilized mice muscle fibers. *J. Cell Biol.* **140**, 1091-1099.

**Lemasters, J. J., Nieminen, A. L., Qian, T., Trost, L., Elmore, S. P., Nishimura, Y., Crowe, R. A., Cascio, W. E., Bradham, C. A., Brenner, D. A. and Herman, B.** (1998). The mitochondrial permeability transition in cell death: a common mechanism in necrosis, apoptosis and autophagy. *Biochim. Biophys. Acta* **1366**, 177-196.

**Leterrier, F., Rusakov, D. A., Nelson, B. D. and Linden, M.** (1994). Interactions between brain mitochondria and cytoskeleton: evidence for specialized outer membrane domains involved in the association of cytoskeleton-associated proteins to mitochondria in situ and in vitro. *Microsc. Res. Tech.* **27**, 233-261.

**Liobikas, J., Kopustinskiene, D. M. and Toleikis, A.** (2001). What controls the outer mitochondrial membrane permeability for ADP: facts for and against the oncotic pressure. *Biochim. Biophys. Acta* **1505**, 220-225.

**Margineantu, D., Capaldi, R. A. and Marcus, A. H.** (2000). Dynamics of the mitochondrial reticulum in live cells using fourier imaging correlation spectroscopy and digital video microscopy. *Biophys. J.* **79**, 1833-1849.

**Menin, L., Panchichkina, M., Keriel, C., Olivares, J., Braun, U., Seppet, E. K. and Saks, V. A.** (2001). Macrocompartmentation of total creatine in cardiomyocytes revisited. *Mol. Cell. Biochem.* **220**, 149-159.

**Milner, D. J., Mavroidis, M., Weisleder, N. and Capetanaki, Y.** (2000). Desmin cytoskeleton linked to muscle mitochondrial distribution and respiratory function. *J. Cell Biol*. **150**, 1283-1298.

**National Institutes of Health** (1985). *Guide for the Care and Use of Laboratory Animals*. *NIH Publication No. 85-23*. Bethesda, MD, USA: NIH.

**Nozaki, T., Kagaya, Y., Ishide, N., Kitada, S., Miura, M., Nawata, J., Ohno, I., Watanabe, J. and Shirato, K.** (2001). Interaction between sarcomere and mitochondrial length in normoxic and hypoxic rat ventricular papillary muscles. *Cardiovasc. Pathol.* **10**, 125-132.

**Ogata, T. and Yamasaki, Y.** (1997). Ultra-high resolution scanning electron microoscopy of mitochondria and sarcoplasmic reticulum arrangement in human red, white, and intermediate muscle fibers. *Anatom. Rec.* **248**, 214-223.

**Opie, L. H.** (1998). The Heart. In *Physiology, From Cell To Circulation*. Third edition. pp. 43-63. Philadelphia: Lippincott-Raven Publishers.

**Phillips, R. C., George, P. and Rutman, R. J.** (1966). Thermodynamic studies of the formation and ionization of the magnesium(II) complexes of ADP and ATP over the pH range 5 to 9. *J. Am. Chem. Soc.* **88**, 2631-2640.

**Rizzuto, R., Pinton, P., Carrington, W., Fay, F. S., Fogarty, K. E., Lifshitz, L. M., Tuft, R. A. and Pozzan, T.** (1998). Close contacts with the endoplasmic reticulum as determinants for mitochondrial $Ca^{2+}$ responses. *Science* **280**, 1763-1766.

**Saks, V. A., Chernousova, G. B., Gukovsky, D. E., Smirnov, V. N. and Chazov, E. I.** (1975). Studies of energy transport in heart cells. Mitochondrial isoenzyme of creatine phosphokinase: kinetic properties and regulatory action of $Mg^{2+}$ ions. *Eur. J. Biochem*. **57**, 273-290.

**Saks, V. A., Belikova, Yu. O. and Kuznetsov, A. V.** (1991). *In vivo* regulation of mitochondrial respiration in cardiomyocytes: Specific restrictions for intracellular diffusion of ADP. *Biochim. Biophys. Acta* **1074**, 302-311.

**Saks, V. A., Vassilyeva, E. V., Belikova, Yu. O., Kuznetsov, A. V., Lyapina, S. A., Petrova, L. and Perov, N. A.** (1993). Retarded diffusion of ADP in cardiomyocytes: Possible role of outer mitochondrial membrane and creatine kinase in cellular regulation of oxidative phosphorylation. *Biochim. Biophys. Acta* **1144**, 134-148.

**Saks, V. A., Khuchua, Z. A., Vasilyeva E. V., Belikova, Y. O. and Kuznetsov, A.** (1994). Metabolic compartmentation and substrate channeling in muscle cells. Role of coupled creatine kinases in *in vivo* regulation of cellular respiration. A synthesis. *Mol. Cell. Biochem.* **133/134**, 155-192.

**Saks, V. A., Kuznetsov, A. V., Khuchua, Z. A., Vasilyeva, E. V., Belikova, Y. O., Kesvatera, T. and Tiivel, T.** (1995). Control of cellular respiration *in vivo* by mitochondrial outer membrane and by creatine kinase. A new speculative hypothesis: possible involvement of mitochondrial–cytoskeleton interactions. *J. Mol. Cell. Cardiol.* **27**, 625-645.

**Saks, V. A., Veksler, V. I., Kuznetsov, A. V., Kay, L., Sikk, P., Tiivel, T., Tranqui, L., Olivares, J., Winkler, K., Wiedemann, F. and Kunz, W. S.** (1998a). Permeabilized cell and skinned fiber techniques in studies of mitochondrial function *in vivo*. *Mol. Cell. Biochem*. **184**, 81-100.

**Saks, V. A., Dos Santos, P., Gellerich, F. N. and Diolez, P.** (1998b). Quantitative studies of enzyme–substrate compartmentation, functional coupling and metabolic channeling in muscle cells. *Mol. Cell. Biochem.* **184**, 291-307.

**Saks, V. A., Kaambre, T., Sikk, P., Eimre, M., Orlova, E., Paju, K., Piirsoo, A., Appaix, F., Kay, L., Regiz-Zagrosek, V., Fleck, E. and Seppet, E.** (2001). Intracellular energetic units in red muscle cells. *Biochem. J*. **356**, 643-657.

**Seppet, E., Kaambre, T., Sikk, P., Tiivel, T., Vija, H., Kay, L., Appaix, F., Tonkonogi, M., Sahlin, K. and Saks, V. A.** (2001). Functional complexes of mitochondria with MgATPases of myofibrils and sarcoplasmic reticulum in muscle cells. *Biochim. Biophys. Acta*, **1504**, 379-395.

**Smirnova, E., Shurland, D. L., Ryazantsev, S. N. and van der Blick, A. M.** (1998). A human dynamin-related protein controls the distribution of mitochondria. *J. Cell Biol*. **143**, 351-359.

**Tiivel, T., Kuznetsov, A., Kadaya, L., Käämbre, T., Peet, N., Sikk, P., Braun, U., Ventura Clapier, R., Saks, V. and Seppet, E. K.** (2000). Developmental changes in regulation of mitochondrial respiration by ADP and creatine in rat heart in situ. *Mol. Cell. Biochem*. **208**, 119-128.

**Toleikis, A., Liobikas, J., Trumbeckaite, S. and Majiene, D.** (2001). Relevance of fatty acid oxidation in regulation of the outer mitochondrial membrane permeability for ADP. *FEBS Lett*. **509**, 245-249.

**Veksler, V. I., Kuznetsov, A. V., Sharov, V. G., Kapelko, V. I. and Saks, V. A.** (1987). Mitochondrial respiratory parameters in cardiac tissue: a novel method of assessment by using saponin-skinned fibers. *Biochim. Biophys. Acta* **892**, 191-196.

**Veksler, V. I., Kuznetsov, A. V., Anflous, K., Mateo, P., van Deursen, J., Wieringa, B. and Ventura-Clapier, R.** (1995). Muscle creatine-kinase deficient mice. II Cardiac and skeletal muscles exhibit tissue-specific adaptation of the mitochondrial function. *J. Biol. Chem*. **270**, 19921-19929.

**Vendelin, M., Kongas, O. and Saks, V. A.** (2000). Regulation of mitochondrial respiration in heart cells analyzed by reaction-diffusion model of energy transfer. *Am. J. Cell Physiol.* **278**, C747-C764.

**Vignais, P.** (1976). Molecular and physiological aspects of adenine nucleotide transport in mitochondria. *Biochim. Biophys. Acta* **456**, 1-38.

**Wallimann, T., Wyss, M., Brdiczka, D., Nicolay, K. and Eppenberger, H.** (1992). Transport of energy in muscle: the phosphorylcreatine shuttle. *Biochem. J.* **281**, 21-40.

**Walsh, B., Tonkonogi, M., Soderlund, K., Hultman, E., Saks, V. and Sahlin, K.** (2001). The role of phosphorylcreatine and creatine in the regulation of mitochondrial respiration in human skeletal muscle. *J. Physiol*. **537**, 971-978.

**Weiss, J. N. and Korge, P.** (2001). The Cytoplasm. No longer a well-mixed bag. *Circ. Res*. **89**, 108-110.

**Williamson, J. R., Ford, C., Illingworth, J. and Safer, B.** (1976). Coordination of cyclic acid cycle activity with electron transport flux. *Circ. Res*. **38** (**Suppl. I)**, 39-51.

**Wyss, M. and Kaddurah-Daouk, R.** (2000). Creatine and creatinine metabolisme. *Physiol. Rev*. **80**, 1107-1213.

**Yaffe, M. P.** (1999). The machinery of mitochondrial inheritance and behaviour. *Science* **283**, 1493-1497.

**Yamashita, H., Sata, M., Sugiura, S., Momomura, S., Serizawa, T. and Iizuka, M.** (1994). ADP inhibits the sliding velocity of fluorescent actin filaments on cardiac and skeletal myosins. *Circ. Res*. **74**, 1027-1033.